
Assessing real options in urban surface water flood risk management under climate change

Haixing Liu^a, Yuntao Wang^{a,b*}, Chi Zhang^a, Albert S. Chen^b, Guangtao Fu^b

^a School of Hydraulic Engineering, Dalian University of Technology, Dalian 116024, China

^b Centre for Water Systems, College of Engineering, Mathematics and Physical Sciences, University of Exeter, North Park Road, Harrison Building, Exeter EX4 4QF, UK

*Corresponding author: Yuntao Wang, E-mail address: wangyuntao@mail.dlut.edu.cn

Abstract: Developing an adaptation option is challenging for long-term engineering decisions due to uncertain future climatic conditions; this is especially true for urban flood risk management. This study develops a real options approach to assess adaptation options in urban surface water flood risk management under climate change. This approach is demonstrated using a case study of Waterloo in London, UK, in which three Sustainable Drainage System (SuDS) measures for surface water flood management, i.e., green roof, bio-retention and permeable pavement are assessed. A trinomial tree model is used to represent the change in rainfall intensity over future horizons (2050s and 2080s) with the climate change data from UK Climate Projections 2009. A two-dimensional Cellular Automata based model CADDIES is used to simulate surface water flooding. The results from the case study indicate

24 that the real options approach is more cost effective than the fixed
25 adaptation approach. The benefit of real options adaptations is found to
26 be higher with an increasing cost of SuDS measures compared to fixed
27 adaptation. This study provides new evidence on the benefits of real
28 options analysis in urban surface water flood risk management given the
29 uncertainty associated with climate change.

30 Key words: Real options; Flood risk; Climate change; Adaptation
31 measures; NPV; SuDS

32 **1. Introduction**

33 Urban surface water flooding, as one of the major natural hazards in
34 both developed and developing countries, can cause great environmental
35 and economic damage and social interruption ([Zhou *et al.* 2012](#);
36 [Hirabayashi *et al.* 2013](#); [Yin *et al.* 2015](#); [Jenkins *et al.* 2017](#); [Löwe *et al.*](#)
37 [2017](#)). For example, the summer floods of 2007 in UK led to 55,000
38 properties flooded with an estimated economic loss of £3.2 billion ([Pitt](#)
39 [2008](#)). This situation can get worse over the next decades due to climate
40 change and rapid urbanization ([Dawson *et al.* 2008](#); [Jenkins *et al.* 2017](#)).
41 The expected annual damage (EAD) from surface water flooding in
42 England can increase by 135% by 2080 under future climate scenario
43 ([Sayers *et al.* 2015](#)). Therefore, there is a need to assess the impact of
44 climate change and develop effective adaptation measures in response to

45 increasing flood risk (Koukoui *et al.* 2015; Zhang *et al.* 2017).

46 Significant efforts have been made during the last few decades to
47 develop cost-effective, long-term adaptation measures for alleviating
48 increased flood risk through cost benefit analysis (Löwe *et al.* 2017). For
49 example, Koukoui *et al.* (2015) described a tipping point-opportunity
50 method to identify the adaptation strategy with lower costs, considering
51 the effects of climate change. Zhou *et al.* (2012) developed a pluvial
52 flood risk assessment framework to identify and access adaptation
53 measures based on the cost-benefit process. Löwe *et al.* (2017) developed
54 a new framework to assess flood risk adaptation measures by coupling a
55 1D-2D hydrodynamic flood model with an agent-based urban
56 development model to consider the long-term effects of urban
57 development and climate change.

58 However, there are large uncertainties in assessing the long-term
59 performance and benefit of adaptation measures, due to multiple sources
60 of uncertainty such as climate change and land use change (Hino & Hall
61 2017). Furthermore, based on the worst climate change scenario, the
62 investments can be very large over a long-term planning horizon (e.g., 30
63 years), this may lead to overdesign for the uncertainty of climate change.
64 To bridge this gap, real options analysis is introduced in this study to
65 handle the uncertainties in future infrastructure investments and provide
66 decision support for appropriate climate change adaptation.

67 The real options approach originated from the study of financial
68 decision making (Myers 1984). The success of financial options
69 development and application led to the award of Nobel Prize in Economic
70 Sciences to Robert Merton and Myron Scholes in 1997. A real option
71 means the right but not the obligation to take future actions. Thus, unlike
72 the traditional planning approach, which considers only one-off
73 investment option and ignores the flexibility under significant future
74 uncertainties, real options can consider management flexibility and
75 volatility by making changes to an investment when new information
76 comes in the future. Many tools have been developed for the analysis of
77 real options, and most of them are based upon the Black-Scholes model
78 and binominal model, such as binominal and trinomial decision trees
79 (Gersonius *et al.* 2013). Apart from financial option analysis, real options
80 is also an important analytical tool that has been applied to a number of
81 diverse fields such as management of infrastructure systems, renewable
82 energy and water supply. For example, Zhao *et al.* (2004) used real
83 options for decision making in highway development, operation,
84 expansion and rehabilitation. Jeuland and Whittington (2014) developed a
85 methodology for planning new water resources infrastructure investment
86 and operating strategies considering climate change uncertainty. Kim *et al.*
87 (2017b) proposed a real options-based framework to assess economic
88 benefits of adapting hydropower plants to climate change.

89 In recent years, the concept of real options has been used in the flood
90 risk management for developing cost-effective adaptation measures in
91 order to reduce the consequences of climate change. [Woodward *et al.*](#)
92 [\(2011\)](#) assessed a set of interventions in a flood system across a range of
93 future climate change scenarios. Furthermore, [Woodward *et al.* \(2014\)](#)
94 developed a new methodology by capturing the concepts of real options
95 and multiobjective optimization to evaluate potential flood risk
96 management opportunities. [Hino and Hall \(2017\)](#) analyzed real options in
97 flood risk management by considering the joint effects of uncertainties in
98 socioeconomic drivers and climate change. However, all these studies
99 above focused on the design of flood defense systems (more specifically
100 on flood walls). In urban flooding, however, there were only a few studies
101 on the use of real options to build flexibility into urban drainage
102 infrastructure ([Gersonius *et al.* 2013](#); [Kim *et al.* 2017a](#)). There is a need
103 to further develop the real options approach in urban surface water flood
104 management and test its effectiveness in developing adaptation measures
105 related to Sustainable Drainage Systems (SuDS).

106 In this paper, we aim to present a real options approach for urban
107 surface water flood risk management under long-term climate change
108 scenarios. The trinomial tree model is used to represent the future
109 changes in rainfall intensity over two planning horizons in 2050 and 2080.
110 The Cellular Automata Dual-DraInagE Simulation (CADDIES) model

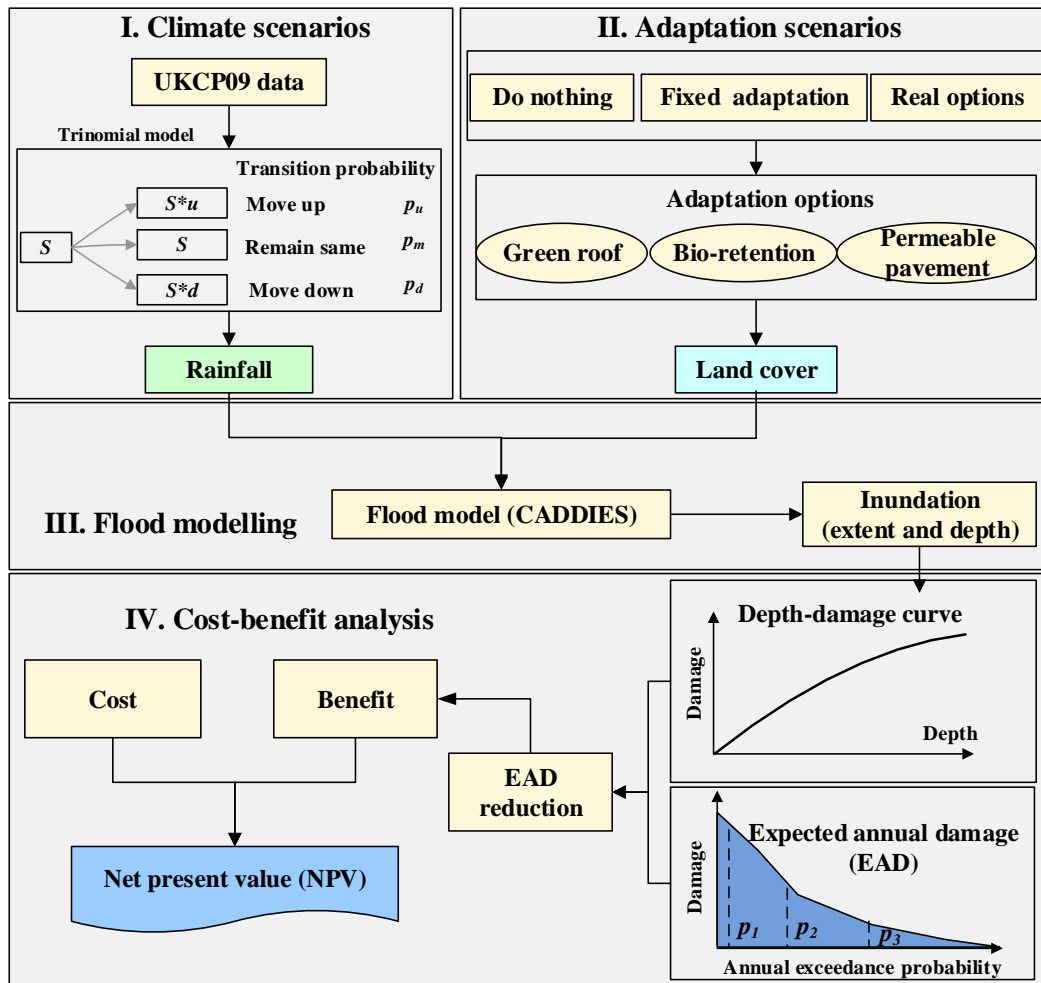
111 (Guidolin *et al.* 2016) is used for flood simulation. The Waterloo urban
112 catchment in London is used as a case study to assess SuDS measures for
113 surface water flood management including green roof, bio-retention and
114 permeable pavement. Real options measures are compared to a fixed
115 adaptation approach. The results obtained from the case study show the
116 advantage of real options in urban surface water flood risk management
117 considering future climate change.

118 **2. Methodology**

119 Fig. 1 summarizes the real options approach used in this study. The
120 climate change data from UKCP09 (Murphy *et al.* 2009) are used to
121 generate climate change scenarios. To investigate the performance of the
122 real options approach on flood risk reduction under future climate change,
123 two different adaptation approaches (i.e. ‘do nothing’ baseline and fixed
124 adaptation approach) are used for comparison with the real options
125 approach through cost-benefit analysis. Furthermore, three kinds of SuDS
126 measures, i.e., green roof, bio-retention and permeable pavement, are
127 chosen to generate adaptation scenarios. The depth-damage curves
128 combined with the inundation (extent and depth) from CADDIES flood
129 model are used to assess flood damage. These are detailed below.

130

131



132

133 **Fig. 1.** The real options approach for assessing the performance of different
 134 adaptation measures.

135 2.1. Climate change scenarios

136 The trinomial tree model, which is an extension of the lattice
 137 binomial model (Boyle 1988), is used to represent the uncertainty of
 138 rainfall due to climate change. This model was originally developed for
 139 real options analysis in financial investments, but has been used in many
 140 fields due to its flexibility and effectiveness, such as renewable energy
 141 and urban drainage infrastructure (Gersonius *et al.* 2013; Dittrich *et al.*
 142 2016; Gong & Li 2016; Tang *et al.* 2017). In this model, the stochastic

143 process is simplified by three jump parameters (u for moving up, d for
 144 moving down and m for remaining the same) to describe the possible
 145 changes of a system's status with related transition probabilities (p_u , p_d
 146 and p_m) over a time period. Meanwhile, these parameters and their
 147 corresponding probabilities can be calculated by Eqs. (1) ~ (6)
 148 (Zaboronski & Zhang 2008).

$$149 \quad p_u = \left(\frac{e^{\frac{r\Delta t}{2}} - e^{-\sigma\sqrt{\frac{\Delta t}{2}}}}{e^{\sigma\sqrt{\frac{\Delta t}{2}}} - e^{-\sigma\sqrt{\frac{\Delta t}{2}}}} \right)^2 \quad (1)$$

$$150 \quad p_d = \left(\frac{e^{\sigma\sqrt{\frac{\Delta t}{2}}} - e^{\frac{r\Delta t}{2}}}{e^{\sigma\sqrt{\frac{\Delta t}{2}}} - e^{-\sigma\sqrt{\frac{\Delta t}{2}}}} \right)^2 \quad (2)$$

$$151 \quad p_m = 1 - p_u - p_d \quad (3)$$

$$152 \quad u = e^{\sigma\sqrt{2\Delta t}} \quad (4)$$

$$153 \quad d = e^{-\sigma\sqrt{2\Delta t}} \quad (5)$$

$$154 \quad m = 1 \quad (6)$$

155 where r is drift rate, σ is the volatility and Δt is the length of the time
 156 period.

157 It is possible to estimate the change of the future rainfall intensity
 158 with u , d and m . Further, when a system's status remains same, i.e., the
 159 rainfall intensity won't change over a time period, so the value of m is set
 160 as 1. For example, the rainfall intensity is denoted by S at time t_0 , then it
 161 will change to $S*u$, $S*d$ or S for each climate change scenario at time t_1 .
 162 Based on the mean and standard deviation of the normal approximation

163 of the climate change data from UKCP09, the drift rate r and volatility σ
164 can be estimated for the change in rainfall intensity by Eqs.(7)~(8)
165 (Gersonius *et al.* 2013), as below:

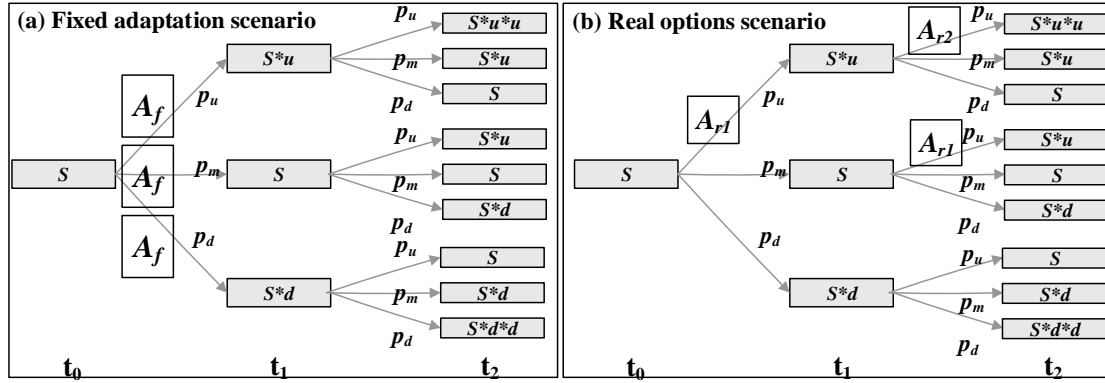
$$166 \quad r = \frac{(\mu-1)}{T} \quad (7)$$

$$167 \quad \sqrt{T}\sigma = \frac{\ln\left(\frac{\mu+2\sigma_s}{\mu}\right)}{2} \quad (8)$$

168 where μ is the mean value for normal approximation of the rainfall
169 change of T years, and σ_s is the standard deviation.

170 **2.2. Approach for adaptation**

171 The real options approach is compared with the traditional fixed
172 adaptation approach. In the fixed adaptation approach, as shown in Fig. 2,
173 all adaptation measures A_f are implemented at year t_0 regardless of future
174 climate predictions. For the real options approach, adaptation measures
175 are adopted only for the scenarios in which the rainfall intensity increases.
176 For example, adaptation measures of A_{r1} will be implemented when the
177 rainfall intensity increases following the upward path with a probability
178 of p_u at year t_0 , then A_{r1} (with a probability of $p_m p_u$) or A_{r2} (with a
179 probability of $p_u p_u$) will be implemented at year t_1 depending on different
180 scenarios of rainfall prediction at year t_2 .



181

182 **Fig. 2.** The diagram of trinomial tree model and overview of intervention approaches
 183 for fixed adaptation scenario and real options scenario. A_f represents the adaptation
 184 measures used in fixed adaptation scenario, and A_{r1} or A_{r2} represents the adaptation
 185 measures used in the real options scenario.

186 **2.3. Flood risk assessment**

187 **2.3.1. Flood modelling**

188 In this paper, the CADDIES model was used for the surface water
 189 mapping to assess the flood risk. CADDIES is a fast 2D urban flood
 190 simulation model for high resolution or large scale simulations based on
 191 the principle of cellular automata (CA). This model performs a 2D pluvial
 192 flood inundation simulation using simple transition rules for modeling
 193 complex physical systems. Furthermore, the model allows each grid cell
 194 using its own roughness value or infiltration rate to represent spatial
 195 variations of land cover condition, soil infiltration and drainage capacity.
 196 This model's effectiveness has been proven on the 2D benchmark test
 197 cases and real world case studies (Guidolin *et al.* 2016).

2.3.2. Flood risk assessment

Expected annual damage (EAD) is often used to evaluate the benefits for adaptation measures in flood risk management decision making, especially for a long-term flood risk intervention strategy (Woodward *et al.* 2011; Zhou *et al.* 2012; Woodward *et al.* 2014; Hino & Hall 2017; Löwe *et al.* 2017). EAD is the frequency weighted sum of damage for the full range of possible damaging flood events and would occur in a particular area over a very long period of time, which can be defined as below:

$$EAD = \int_0^1 D(p) dp \quad (9)$$

where D is the flood damage and p is the annual exceedance probability for a rainfall event.

In this paper, we consider the direct tangible flood damages on building to quantify the impact of flooding and the benefits of implementing different adapting strategies. The damage is determined using the flood depth information obtained from CADDIES and the depth-damage functions for different building uses. Furthermore, the trapezoidal rule (Olsen *et al.* 2015) is used to approximate the EAD using three events. For example, three rainfall events with the annual exceedance probability of p_1 , p_2 and p_3 are illustrated to calculate the damage in Fig. 1.

219 For each adaptation scenario, the total damage is calculated by
220 integration of the flood damages over all different rainfall paths with
221 different probabilities. So even with the same adaptation measures
222 implemented in year 2080, the EAD will be different in the fixed and real
223 options approaches due to the probabilities of future climate scenarios
224 considered in Equation (9).

225 **2.4. Cost benefit analysis**

226 In order to compare the benefits of different adaptation investments
227 with the corresponding costs, cost-benefit analysis is implemented to
228 assess the performance of real options in flood risk reduction compared to
229 the fixed adaptation approach and ‘do nothing’ baseline. The benefits are
230 defined as the reduction in flood damage when the adaptation
231 implemented compared to the baseline scenario without adaptation. The
232 investment costs of adaptation measures can be obtained for green roof,
233 bio-retention and permeable pavement. NPVs are calculated with a
234 discount rate in order to convert the benefits and costs at different future
235 horizons to their present values using the equation below:

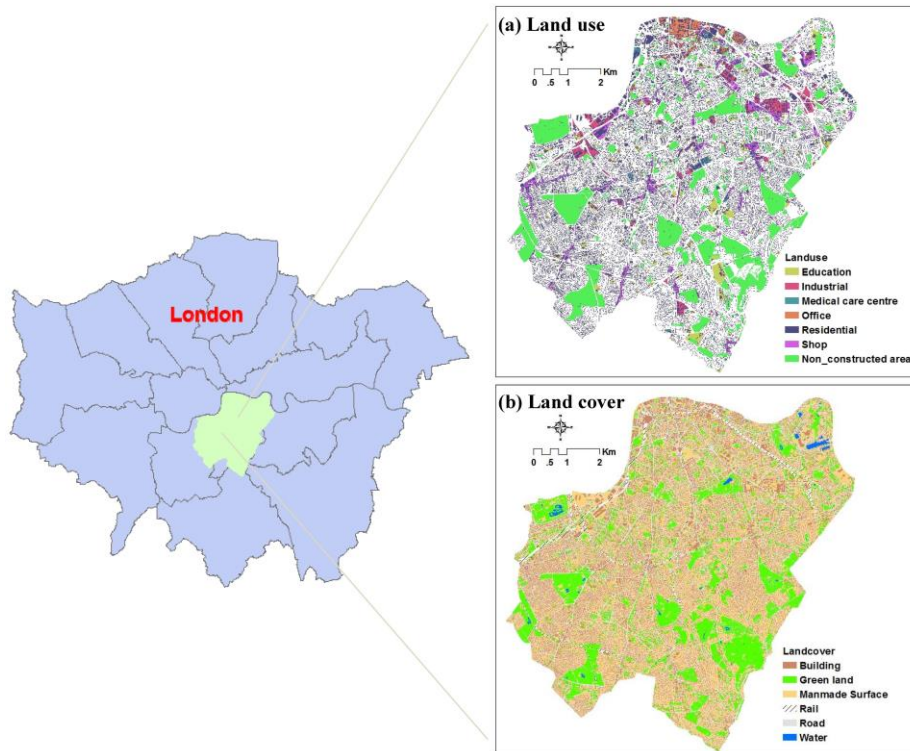
$$236 \quad NPV = \sum_{t=0}^T \frac{(B_t - C_t)}{(1+r)^t} \quad (10)$$

237 where B_t represents the benefits of the adaptation measure at year t , C_t
238 is the cost of the adaptation measure at year t , r denotes the discount rate
239 and T is the total number of years considered. Higher NPV values

240 indicate that the relevant adaptation approaches are more cost effective in
241 alleviating the increased flood risk.

242 3. Case study

243 3.1. Study area



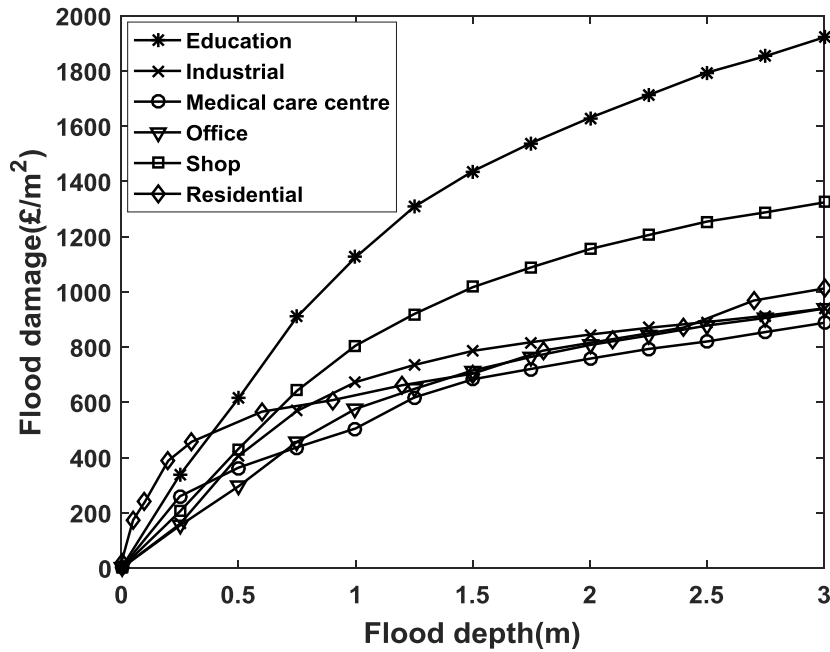
244

245 **Fig. 3.** Location, land cover and land use maps for the study area.

246 In this paper, the Waterloo area in the London Borough of
247 Southwark is used as the case study. The digital elevation data (DEM) of
248 bare terrain, obtained from Ordnance Survey, has a $5\text{ m} \times 5\text{ m}$ resolution
249 with the highest and lowest elevations of 115.5 m and -6.4 m, respectively.
250 We analyzed the terrain elevation to determine the catchment boundary of
251 the study area, and thus the closed boundary condition was set in the
252 flood model.

253 As shown in Fig. 3(b), the topography data ([Ordnance Survey 2015](#))
254 was classified into six different land cover types, including building,
255 green land, manmade surface, rail, road and water, to set up the
256 infiltration rate and roughness parameters in the CADDIES flood model.
257 The Waterloo catchment covers an area of 68.8 km², with 81.0%
258 developed as buildings and impervious surfaces, while 19.0% of the area
259 remains as permeable green land.

260 Furthermore, this study area can also be classified into seven
261 different land use types, including education, industrial, medical care
262 center, office, residential, shop and non_constructed areas (Fig. 3(a)), for
263 assessing direct tangible flood damages based on the depth-damage
264 functions. The depth-damage functions are available for over 100
265 building types in the UK's Multi-coloured Manual ([Penning-RowSELL *et al.* 2010](#)).
266 Fig. 4 shows the depth-damage functions of the six land use
267 types considered in this study.

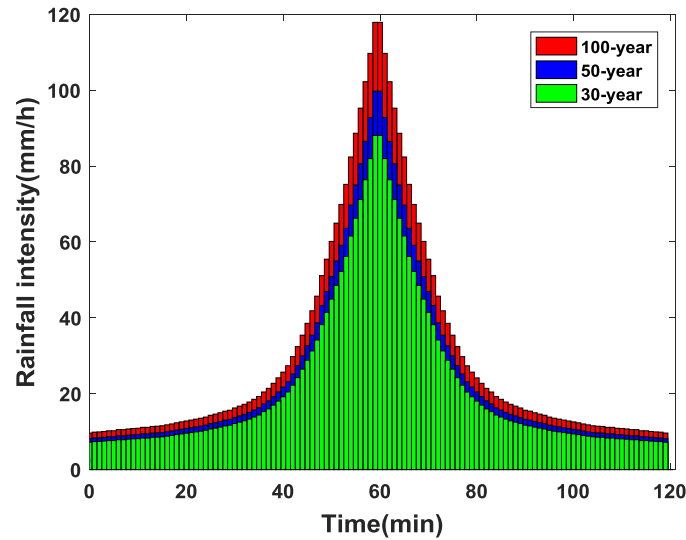


268
269 **Fig. 4.** Depth-damage functions for six land use types.

270 **3.2. Rainfall events**

271 **3.2.1 Design rainfall**

272 In order to calculate the EAD under different adaptation scenarios,
 273 design rainfall events of three return periods (30-, 50- and 100-year
 274 events) with a duration of 2h were simulated using the rainfall
 275 Intensity-Duration-Frequency curves from the Flood Estimation
 276 Handbook (CEH 2015), and the rainfall hyetographs are shown in Fig. 5.
 277 Furthermore, the design rainfall depths and peak rainfall intensities under
 278 different return periods are shown in Table 1.



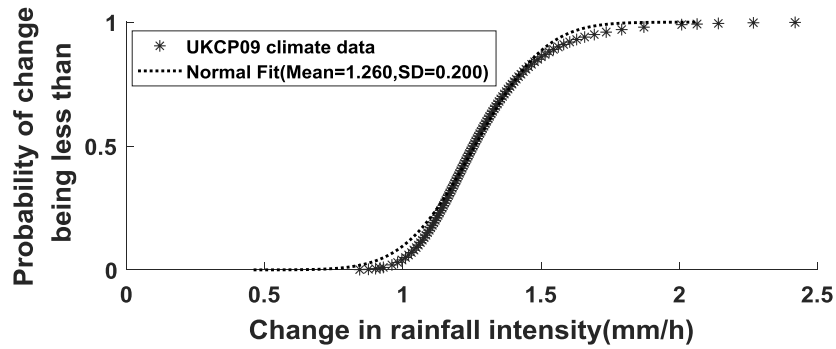
279
280 **Fig. 5.** Design rainfalls with 30-, 50- and 100-year return periods.

281 **Table 1.** Rainfall depth and peak rainfall intensity of 2-hour design rainfalls for 30-,
282 50- and 100-year return periods.

Return period (year)	Rainfall depth (mm)	Peak rainfall intensity (mm/h)
30	45	88
50	51	100
100	60	118

283 3.2.2 Climate change

284 In this study, the cumulative distribution data of rainfall intensity
285 change (London, UK) by 2080s under high emissions were obtained from
286 UKCP09 (UKCP09 2017), as shown in Fig. 6. Furthermore, a normal
287 distribution (mean $\mu = 1.260$, and standard deviation $\sigma_s = 0.200$) was
288 fitted to the UKCP09 climate data. The drift rate r and volatility σ were
289 calculated as 0.24% and 1.45% using Eqs. (7)~(8).



290
291 **Fig. 6.** Cumulative distribution of change in rainfall intensity

292 Furthermore, a planning horizon from 2020 to 2080 was considered,
293 and the adaptation measures will be applied in two stages, i.e., $t_0 = 2020$,
294 $t_1 = 2050$. With the interval of 30 years, three jump parameters (u , d and
295 m) with related transition probabilities (p_u , p_d and p_m) are estimated as
296 below: $u = 1.12$, $d = 0.89$, $m = 1$, $p_u = 76.9\%$, $p_m = 21.6\%$ and $p_d =$
297 1.5% . Then we can calculate rainfall for the future years of 2050 and
298 2080 based on the three design rainfalls with 30-, 50- and 100-year return
299 periods.

300 **3.3. Adaptation scenarios**

301 SuDS is used to manage flood risk by slowing down and reducing
302 the quantity of surface water runoff (Woods *et al.* 2015). Out of many
303 different SuDS measures for surface water management, we considered
304 three measures in this paper, i.e., green roof implemented for every grid
305 cell of buildings, permeable pavement for every grid cell of roads, and
306 bio-retention for every grid cell of manmade surface. However, as shown
307 in Table 2, we have considered 7 combinations of measures for the fixed

308 adaptation approach and 19 combinations for the real options approach.

309 For example, for the fixed adaptation scenario F5, green roof and
310 permeable pavement will be adopted for every grid cell of each land
311 cover in year $t_0=2020$. For real options scenario R7, adaptation measures
312 G will be implemented in year 2020 when the rainfall intensity is
313 predicted to increase, i.e., following the upward path with a probability of
314 p_u . Then in 2050, adaption measures will be implemented in two cases
315 only: 1) P will be implemented when rainfall intensity is predicted to
316 increase from S^*u to S^*u^*u ; 2) G will be implemented when rainfall
317 intensity is predicted to increase from S to S^*u . So F5 and R7 can have
318 the same measures in 2080 but this is true only when the rainfall intensity
319 increases from S in 2020 to S^*u in 2050 and further to S^*u^*u in 2080. In
320 all other climate change scenarios, F5 and R7 will have different
321 measures implemented in 2080.

322

323

324

325

326

327

328

329

330 **Table 2.** Adaptation scenarios for the fixed adaptation approach and real options
 331 approach. G stands for green roof, B for bio-retention and P for permeable pavement.
 332 The adaption path of A_f , A_{r1} and A_{r2} are shown in Fig. 2.

Fixed adaptation			Real options				
Scenario	A_f	Scenario	A_{r1}	A_{r2}	Scenario	A_{r1}	A_{r2}
F1	G	R1	B	-	R11	P	G
F2	B	R2	B	G	R12	P	GB
F3	P	R3	B	P	R13	GB	-
F4	GB	R4	B	GP	R14	GB	P
F5	GP	R5	G	-	R15	GP	-
F6	BP	R6	G	B	R16	GP	B
F7	GBP	R7	G	P	R17	BP	-
		R8	G	BP	R18	BP	G
		R9	P	-	R19	GBP	-
		R10	P	B			

333

334 Table 3 shows the unit costs for each SuDS measures below:
 335 £50~90/m² for green roof, £15~35/m² for bio-retention and £20~40/m²
 336 for permeable pavement (HaskoningDHV 2012; Environment Agency
 337 2015). The unit cost of £70/m², £25/m² and £30/m² are chosen for green
 338 roof, bio-retention and permeable pavement. The discount rate was
 339 applied according to HM Treasury guidance, i.e., 3.5% for the years
 340 between 2020 and 2050, 3.0% for the years between 2050 and 2080
 341 (Treasury & Book 2003).

342 **Table 3.** Cost for the three adaptation measures

Measures	Green roof	Bio-retention	Permeable pavement	
Unit cost	Lower	50	15	20
(£/m ²)	Average	70	25	30
	Upper	90	35	40

3.4. Flood simulation details

In CADDIES, different Manning's roughness values were assigned to different land cover types: (1) 0.05 s/m^{1/3} for the building areas; (2) 0.03 s/m^{1/3} for green lands; (3) 0.025 s/m^{1/3} for manmade surface areas; (4) 0.05 s/m^{1/3} for rails; (5) 0.02 s/m^{1/3} for roads; and (6) 0.035 s/m^{1/3} for water (Environment Agency 2013).

Furthermore, different constant infiltration rates were applied to different land covers to reflect both urban drainage capacity and soil infiltration. The combined sewer drainage system was designed to accommodate a rainfall event of the 15 year return period in the London Borough of Southwark (Environment Agency 2011). A combination of infiltration rates, i.e., 35 mm/h and 25 mm/h, were set for the green land cover and other covers during the model setup process according to the drainage capacity.

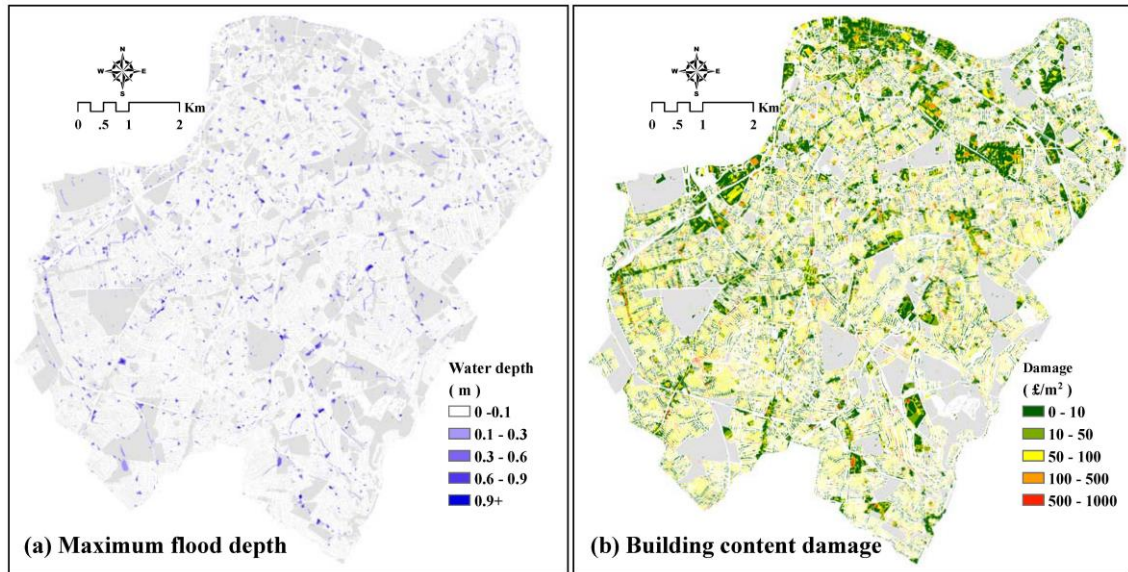
Note that this study is to illustrate the performance of real options on flood damage reduction rather than produce the exact reduction of runoff. Thus, infiltration rates for the land covers of building, manmade surface and road are assumed to be increased by 12 mm/h, 5 mm/h and 8 mm/h when green roof, bio-retention and permeable pavement are adopted, respectively, according to the literature (Qin *et al.* 2013; Woods *et al.* 2015; Alizadehtazi *et al.* 2016; Jato-Espino *et al.* 2016; Bell *et al.* 2017; Ossa-Moreno *et al.* 2017; Rocheta *et al.* 2017).

365 **4. Results and discussion**

366 **4.1. Expected annual damage**

367 The maximum flood depth and damage under the design rainfall of
368 30-year return period are presented in Fig. 7. The damage values shown
369 in Fig. 7(b) are the direct building content damage per unit area.
370 Extensive flood is distributed over the grid cells of building, road,
371 manmade surface and so on. For example, the inundation extent
372 (depth>0.1m) would cover a total area of 2.3 km², of which the grid cells
373 of building account for 23%. Furthermore, the inundation depth in 130
374 grid cells of building is greater than 1.0 metre.

375 The total building flood damage for the study area can be calculated
376 based on the unit damages. The EAD is then calculated by integration of
377 the flood damage over the three rainfall events, each with a specific
378 probability. In this study, the EAD for 2020, 2050 and 2080 are calculated,
379 and for other years the EAD is calculated using linear interpolation.

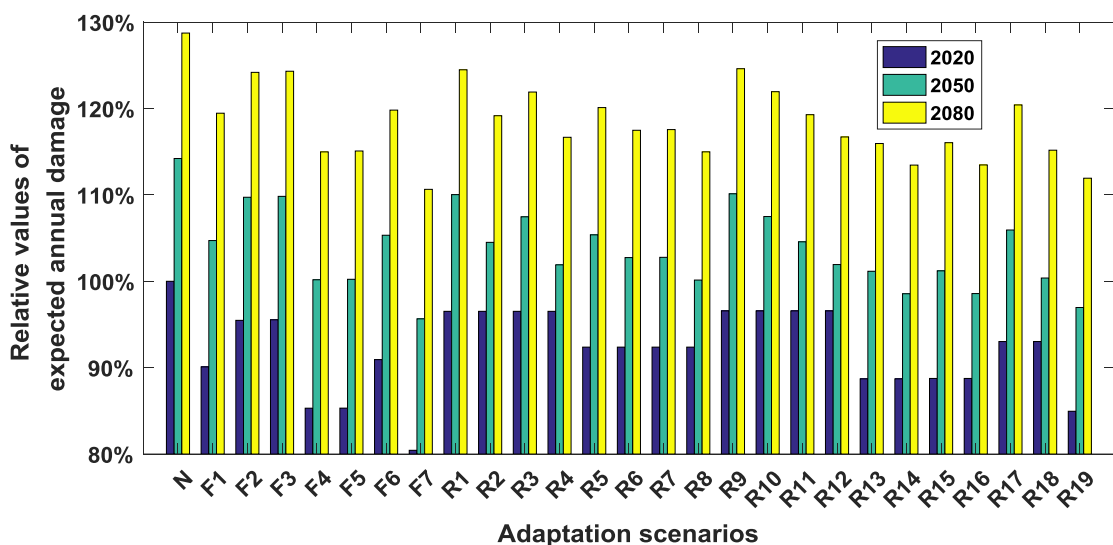


380
 381 **Fig. 7.** Maximum flood depth and direct building content damage per unit area under
 382 the 30-year design rainfall.

383 The EADs are simulated for the real options, the fixed adaptation
 384 and the ‘do nothing’ baseline case. Compared with EAD for 2020 under
 385 ‘do nothing’ scenario, relative values of EAD for 2020, 2050 and 2080
 386 under different adaptation scenarios are presented in Fig. 8. The EAD of
 387 the ‘do nothing’ baseline case increases rapidly from 2020 to 2080 due to
 388 increased rainfall intensities. Specifically, EADs are $£29.2 \times 10^6$, $£33.4$
 389 $\times 10^6$ and $£37.6 \times 10^6$ for year 2020, 2050 and 2080 under the ‘do nothing’
 390 baseline case, i.e., relative EADs are 100%, 114%, 129%. However, the
 391 seven fixed adaptation scenarios can effectively reduce the EAD in a
 392 range of different values. The implementation of SuDS measures is
 393 effective in reducing flood risk, even though flood risk still increases in
 394 the planning horizon as a result of increased rainfall intensities. For
 395 example, in F1, the relative EAD is reduced to 90% in 2020 when
 396 compared to 100% in the base case, due to the green roof measure

397 adopted, but increases to 105% and 119% in 2050 and 2080, respectively.
 398 It is clear that scenario F7 is the most effective amongst the fixed
 399 scenarios, because all three measures are adopted at year 2020, with the
 400 smallest relative EAD for the year 2050 and 2080, i.e., 96% and 111%,
 401 respectively.

402 The 19 real options scenarios show a similar trend to the fixed
 403 adaptation approach between year 2020 and 2050 and the EADs are
 404 further reduced when adaptation measures are adopted at year 2050.
 405 However, when same measures are adopted, the real options approach
 406 tends to result in a slightly larger EAD than the fixed adaptation approach.
 407 This is because these adaptation measures are only implemented when the
 408 rainfall increases following the upward path. For example, relative EADs
 409 are 96% and 111% for year 2050 and 2080 under the scenario of F7, but
 410 they are 97% and 112% under the scenario of R19, though both scenarios
 411 consider three kinds of adaptation measures in the planning horizon.



412

413 **Fig. 8.** Relative values of expected annual damage for 2020, 2050 and 2080 under
414 different adaptation scenarios compared with expected annual damage for 2020 under
415 'do nothing' scenario. N represents 'do nothing' baseline case.

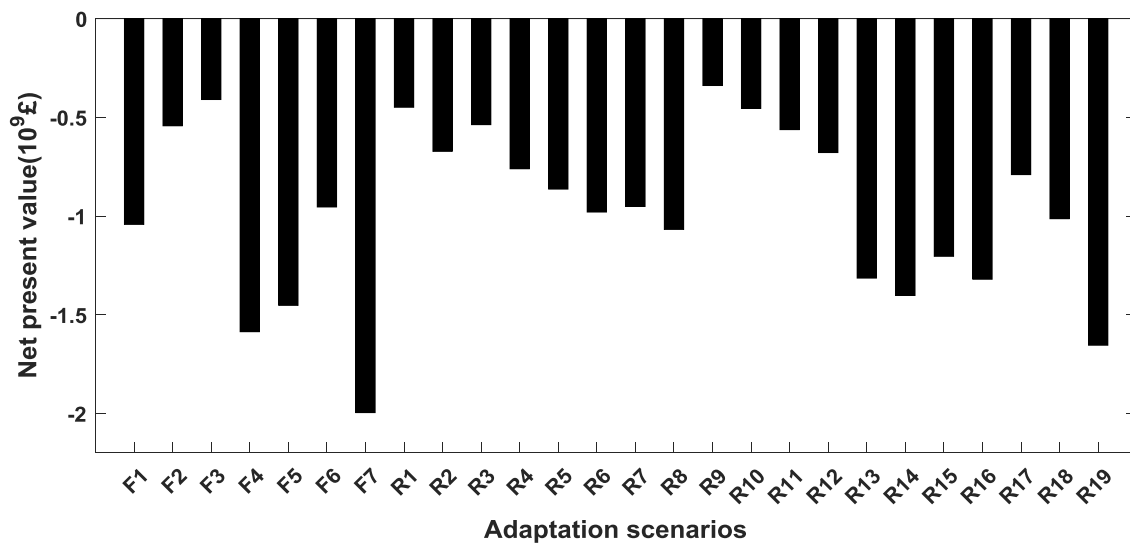
416 **4.2. Net present value**

417 Cost-benefit analysis is conducted to compare different adaptation
418 approaches. The benefit of an adaptation measure can be calculated as the
419 difference between the EADs before and after the adaptation adopted.

420 Fig. 9 shows NPVs for the 7 fixed adaptation scenarios and 19 real
421 options scenarios. In the fixed adaptation scenarios, F7 has the smallest
422 NPV, $-\pounds 2.00 \times 10^9$, even though it has the largest benefit (reduced EAD).
423 This is related to the high cost of F7 due to the implementation of all
424 three kinds of adaptation measures regardless of the future climate.
425 Furthermore, the real options approach has higher NPV than fixed
426 adaptation approach by adopting the same measures in the planning
427 horizon when the rainfall increases following the upward path. For
428 example, both F7 and R19 consider the same SuDS measures, but their
429 NPVs are $-\pounds 2.00 \times 10^9$ and $-\pounds 1.02 \times 10^9$, respectively. This implies that the
430 real options approach is substantially more cost effective than fixed
431 adaptation approach.

432 The results in Fig. 9 show that all the calculated NPVs of the fixed
433 adaptation and real options are negative. This is because only direct
434 tangible damage to buildings is considered in this study. However, more
435 benefits can be provided from flood reduction due to the adoption of

436 SuDS measures. For example, economic benefits can arise from reduced
 437 road damage, basement damage, sewer damage and traffic delays.
 438 Furthermore, SuDS can also provide ecosystem service benefits (wider
 439 benefits), including mitigation of heat island effects and noise,
 440 improvements in water and air quality (Ossa-Moreno *et al.* 2017).
 441 Negative NPVs obtained from flood adaptation assessment are not
 442 uncommon in the literature (Zhou *et al.* 2012; Löwe *et al.* 2017), for
 443 example, Löwe *et al.* (2017) found that the performance of adaptation
 444 strategies strongly depended on many factors, and thus may led to
 445 negative NPVs values.



446
 447 **Fig. 9.** Net present values of 7 fixed adaptation scenarios and 19 real options
 448 scenarios

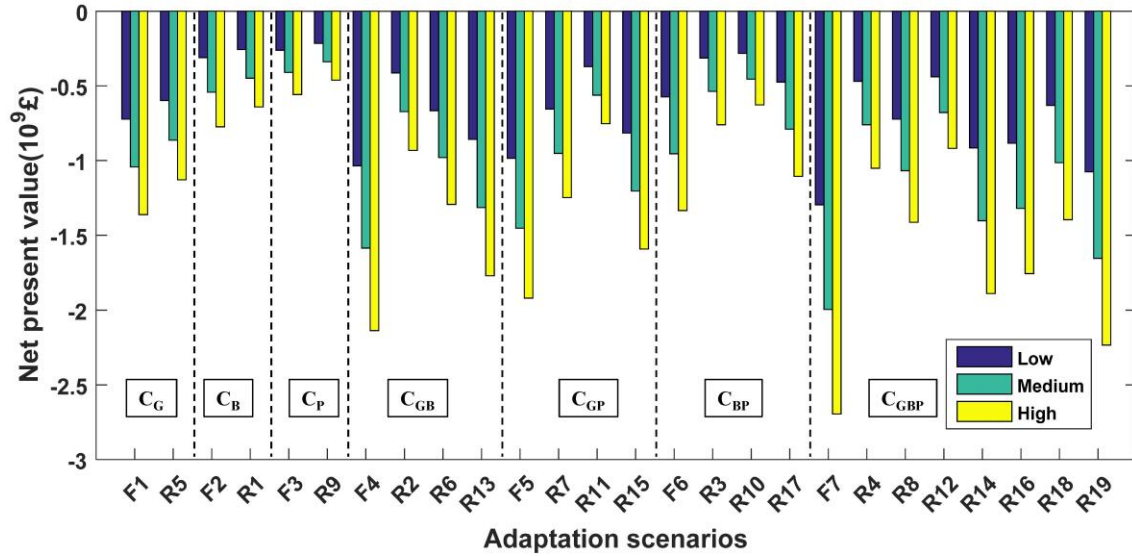
449 4.3. Uncertainty analysis

450 Uncertainties in the adaptation costs and SuDS measures drainage
 451 capacity are considered in the cost-benefit analysis and the results are

452 analysed below.

453 **4.3.1 Adaptation cost uncertainty**

454 In the analyses discussed above, the average costs shown in Table 3
455 are considered. The lower and upper costs were chosen for further
456 analysis. The NPVs of 26 adaptation scenarios under low, medium and
457 high cost scenarios are shown in Fig. 10. The 26 scenarios are divided
458 into 7 categories according to the kind of measures adopted during the
459 planning horizon: C_G , C_B and C_P when only one measure is adopted, C_{GB} ,
460 C_{GP} and C_{BP} when two measures adopted, and C_{GBP} when all three
461 measures adopted. The NPV tends to decrease as the cost of SuDS
462 measures increases. For example, NPVs are $-\pounds 0.72 \times 10^9$, $-\pounds 1.00 \times 10^9$ and
463 $-\pounds 1.36 \times 10^9$ for scenario F1 under low, medium and high cost scenarios,
464 separately. Furthermore, the difference between the fixed adaptation
465 approach and the real options approach in each category increases as the
466 increase of costs. The real options approach has a bigger advantage than
467 the fixed adaptation approach when the cost increases. For example, for
468 the category of C_{GBP} , the differences in NPV between F7 and R18 under
469 low, medium and high cost scenarios are $\pounds 0.67 \times 10^9$, $\pounds 0.98 \times 10^9$ and
470 $\pounds 1.30 \times 10^9$, respectively.

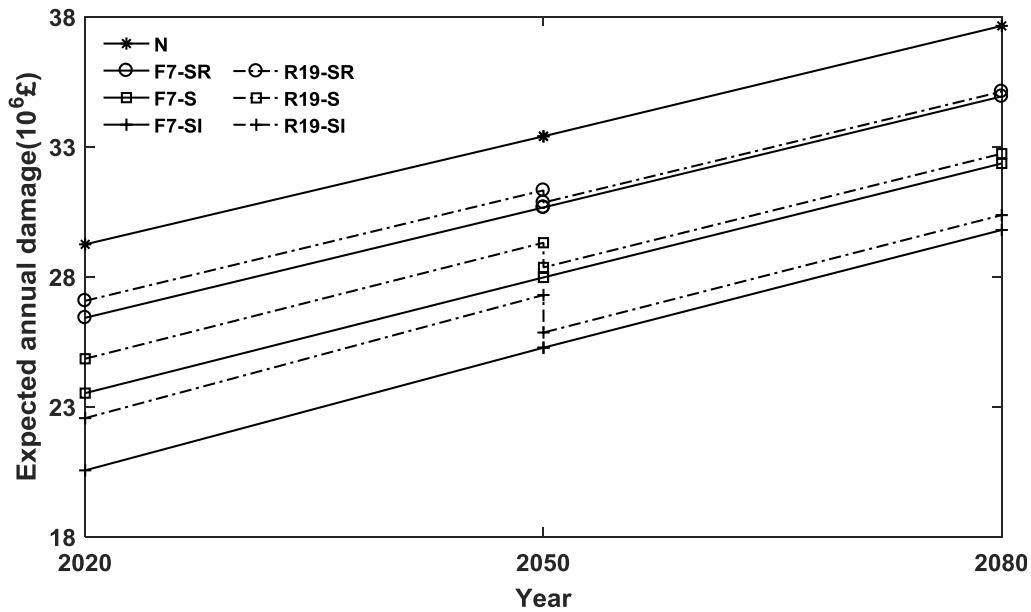


471

472 **Fig. 10.** Net present values under low, medium and high cost scenarios.

473 **4.3.2 SuDS measures drainage capacity uncertainty**

474 In order to study the influence of the uncertainty in drainage
 475 capacity of the SuDS measures, two scenarios of infiltration rate were set
 476 up for flood damage analysis based on the current drainage capacity
 477 (denoted by ‘S’): ‘SR’ represents a 50% reduction of the increased
 478 infiltration rate for SuDS measures of green roof, bio-retention and
 479 permeable pavement, and ‘SI’ represents a 50% increase of the increased
 480 infiltration rate for each SuDS measure. The EAD for fixed adaptation
 481 scenario F7 and real adaptation scenario R19 are shown in Fig. 11.



482
 483 **Fig. 11.** Expected annual damages of adaptation scenarios F7 and R19 under different
 484 drainage capacity scenarios of ‘S’, ‘SR’ and ‘SI’. N represents ‘do nothing’ baseline
 485 case.

486 Fig. 11 illustrates the variations in EAD during the planning horizon
 487 for the adaptation scenarios F7 and R19 under different drainage capacity
 488 scenarios. For fixed adaptation scenario F7, a big difference in flood
 489 damage is shown under the drainage capacity scenario of ‘S’, ‘SR’ and
 490 ‘SI’. That is, EAD values can be reduced when the drainage capacity is
 491 increased. However, EAD values might be higher when the drainage
 492 capacity is reduced under the scenario of ‘SR’.

493 The real option adaptation scenario R19 shows the similar
 494 characteristics to the fixed adaptation F7 though its flood damage is
 495 larger than that of F7. Furthermore, the difference between R19 and F7
 496 tends to become smaller with a decrease in the drainage capacity. For

497 example, the difference of EAD between R19 and F7 are $£2.0 \times 10^6$ and
498 $£0.6 \times 10^6$ for year 2050 and 2080 under ‘SI’, while only $£0.7 \times 10^6$ and
499 $£0.2 \times 10^6$ for ‘SR’.

500 **5. Conclusions**

501 In this paper a real options approach was developed to assess
502 adaptation options in urban surface water flood risk management under
503 climate change. A CA-based urban two-dimensional model was used to
504 simulate surface water flooding. The trinomial tree model was used to
505 calculate the transition probability of rainfall intensity change over the
506 planning horizon with the climate change data from UKCP09. Two
507 approaches, fixed adaptation and real options, were investigated and
508 compared using a case study of the Waterloo catchment in London, UK.
509 Main conclusions are drawn as below:

510 1) The real options approach is more cost effective compared to the
511 fixed adaptation approach. When the same SuDS measures are adopted
512 during the planning horizon, the real options approach can have a slightly
513 higher EAD but have a much lower cost when compared with the fixed
514 approach, which makes it achieve a higher NPV during the planning
515 horizon.

516 2) The real options approach achieves a bigger advantage than the
517 fixed adaptation approach with an increasing cost of adaptation

518 measures but the benefit is reduced when the drainage capacity of SuDS
519 measures decreases.

520 3) The results obtained from the case study indicate the real options
521 approach is able to handle the uncertainty of climate change in assessing
522 SuDS measures for surface water flood risk management.

523 This study considers three SuDS measures only in a case study of
524 the Waterloo catchment. More SuDS measures will be further
525 investigated in the future in order to explore the advantage of using real
526 options on urban surface water flood risk management.

527 **Acknowledgments**

528 This research was partially funded by the British Council through
529 the Global Innovation Initiative (GII206) and the UK Engineering and
530 Physical Sciences Research Council under the Building Resilience into
531 Risk Management project (EP/N010329/1). The corresponding author
532 was funded by the China Scholarship Council. The authors would also
533 like to thank Ordnance Survey for the Master Maps, and NVIDIA
534 Corporation for the Tesla K20c GPU used in this research.

535 **References**

- 536 Alizadehtazi B., DiGiovanni K., Foti R., Morin T., Shetty N. H., Montalto F. A. and Gurian P. L.
537 (2016). Comparison of Observed Infiltration Rates of Different Permeable Urban Surfaces Using a
538 Cornell Sprinkle Infiltrometer. *Journal of Hydrologic Engineering* 21(7), 06016003.
- 539 Bell S., Jones K., McIntosh A., Malki-Epshtein L. and Yao Z. (2017). *Green Infrastructure for*
540 *London: A review of the evidence*, London.
- 541 Boyle P. P. (1988). A lattice framework for option pricing with two state variables. *Journal of*

542 *Financial and Quantitative Analysis* 23(1), 1-12.

543 CEH (2015). FEH Web Service. <https://fehweb.ceh.ac.uk/>.

544 Dawson R., Speight L., Hall J., Djordjevic S., Savic D. and Leandro J. (2008). Attribution of flood
545 risk in urban areas. *Journal of Hydroinformatics* 10(4), 275-88.

546 Dittrich R., Wreford A. and Moran D. (2016). A survey of decision-making approaches for climate
547 change adaptation: Are robust methods the way forward? *Ecological Economics* 122(68), 79-89.

548 Environment Agency (2011). *Surface water management plan-London Borough of Southwark*,
549 Bristol, UK.

550 Environment Agency (2013). *Updated Flood Map for Surface Water-National Scale Surface*
551 *Water Flood Mapping Methodology*, Bristol, UK.

552 Environment Agency (2015). *Cost estimation for SUDS - summary of evidence*, Bristol, UK.

553 Gersonius B., Ashley R., Pathirana A. and Zevenbergen C. (2013). Climate change uncertainty:
554 building flexibility into water and flood risk infrastructure. *Climatic Change* 116(2), 411-23.

555 Gong P. and Li X. (2016). Study on the investment value and investment opportunity of renewable
556 energies under the carbon trading system. *Chinese Journal of Population Resources and Environment*
557 14(4), 271-81.

558 Guidolin M., Chen A. S., Ghimire B., Keedwell E. C., Djordjević S. and Savić D. A. (2016). A
559 weighted cellular automata 2D inundation model for rapid flood analysis. *Environmental Modelling &*
560 *Software* 84(2016), 378-94.

561 HaskoningDHV R. (2012). *Costs and Benefits of Sustainable Drainage Systems*, UK.

562 Hino M. and Hall J. W. (2017). Real Options Analysis of Adaptation to Changing Flood Risk:
563 Structural and Nonstructural Measures. *ASCE-ASME Journal of Risk and Uncertainty in Engineering*
564 *Systems, Part A: Civil Engineering* 3(3), 04017005.

565 Hirabayashi Y., Mahendran R., Koirala S., Konoshima L., Yamazaki D., Watanabe S., Kim H. and
566 Kanae S. (2013). Global flood risk under climate change. *Nature climate change* 3(9), 816-21.

567 Jato-Espino D., Charlesworth S. M., Bayon J. R. and Warwick F. (2016). Rainfall–Runoff
568 Simulations to Assess the Potential of SuDS for Mitigating Flooding in Highly Urbanized Catchments.
569 *International journal of environmental research and public health* 13(1), 149.

570 Jenkins K., Surminski S., Hall J. and Crick F. (2017). Assessing surface water flood risk and
571 management strategies under future climate change: Insights from an Agent-Based Model. *Science of*
572 *The Total Environment* 595(2017), 159-68.

573 Jeuland M. and Whittington D. (2014). Water resources planning under climate change: Assessing
574 the robustness of real options for the Blue Nile. *Water Resources Research* 50(3), 2086-107.

575 Kim K., Ha S. and Kim H. (2017a). Using real options for urban infrastructure adaptation under
576 climate change. *Journal of Cleaner Production* 143(2017), 40-50.

577 Kim K., Park T., Bang S. and Kim H. (2017b). Real Options-Based Framework for Hydropower
578 Plant Adaptation to Climate Change. *Journal of Management in Engineering* 33(3), 04016049.

579 Koukoui N., Gersonius B., Schot P. P. and van Herk S. (2015). Adaptation tipping points and
580 opportunities for urban flood risk management. *Journal of Water and Climate Change* 6(4), 695-710.

581 Löwe R., Urich C., Domingo N. S., Mark O., Deletic A. and Arnbjerg-Nielsen K. (2017).
582 Assessment of urban pluvial flood risk and efficiency of adaptation options through simulations—A new
583 generation of urban planning tools. *Journal of Hydrology* 550(2017), 355-67.

584 Murphy J. M., Sexton D., Jenkins G., Booth B., Brown C., Clark R., Collins M., Harris G.,
585 Kendon E. and Betts R. (2009). *UK climate projections science report: climate change projections*,

586 Report 1906360022, Exeter, UK.

587 Myers S. C. (1984). Finance theory and financial strategy. *Interfaces* 14(1), 126-37.

588 Olsen A. S., Zhou Q., Linde J. J. and Arnbjerg Nielsen K. (2015). Comparing Methods of
589 Calculating Expected Annual Damage in Urban Pluvial Flood Risk Assessments. *Water* 7(1), 255-70.

590 Ordnance Survey (2015). OS MasterMap Topography Layer [FileGeoDatabase geospatial data],
591 Scale 1:1250, Tiles: GB, Updated: 11 June 2015, Ordnance Survey (GB), Using: EDINA Digimap
592 Ordnance Survey Service, <http://digimap.edina.ac.uk>, Downloaded: 2016-02-02.
593 <http://digimap.edina.ac.uk>.

594 Ossa-Moreno J., Smith K. M. and Mijic A. (2017). Economic analysis of wider benefits to
595 facilitate SuDS uptake in London, UK. *Sustainable Cities and Society* 28(2017), 411-9.

596 Penning-Rowsell E., Viavattene C., Pardoe J., Chatterton J., Parker D. and Morris J. (2010). *The*
597 *Benefits of Flood and Coastal Risk Management: A Handbook of Assessment Techniques*, Flood Hazard
598 Research Centre, Middlesex University, London.

599 Pitt M. (2008). *Learning lessons from the 2007 floods*, London: Cabinet Office.

600 Qin H.-p., Li Z.-x. and Fu G. (2013). The effects of low impact development on urban flooding
601 under different rainfall characteristics. *Journal of environmental management* 129(2013), 577-85.

602 Rocheta V. L. S., Isidoro J. M. G. and de Lima J. L. (2017). Infiltration of Portuguese cobblestone
603 pavements—An exploratory assessment using a double-ring infiltrometer. *Urban Water Journal* 14(3),
604 291-7.

605 Sayers P., Horritt M., Penning-Rowsell E. and McKenzie A. (2015). Climate Change Risk
606 Assessment 2017: Projections of future flood risk in the UK. *Research undertaken by Sayers and*
607 *Partners on behalf of the Committee on Climate Change. Published by Committee on Climate Change,*
608 *London.*

609 Tang B.-J., Zhou H.-L., Chen H., Wang K. and Cao H. (2017). Investment opportunity in China's
610 overseas oil project: An empirical analysis based on real option approach. *Energy Policy* 105(2017),
611 17-26.

612 Treasury H. and Book G. (2003). Appraisal and Evaluation in Central Government. *The Stationery*
613 *Office, London.*

614 UKCP09 (2017). <http://ukclimateprojections.metoffice.gov.uk/>.

615 Woods B., Wilson S., Udale-Clarke H., Illman S., Scott T., Ashley R. and Kellagher R. (2015).
616 *The SuDS Manual, C753, CIRIA, London, UK*, ISBN 978-0-86017-760-9. http://www.susdrain.org/resources/SuDS_Manual.html.

617

618 Woodward M., Gouldby B., Kapelan Z., Khu S. T. and Townend I. (2011). Real options in flood
619 risk management decision making. *Journal of Flood Risk Management* 4(4), 339-49.

620 Woodward M., Kapelan Z. and Gouldby B. (2014). Adaptive Flood Risk Management Under
621 Climate Change Uncertainty Using Real Options and Optimization. *Risk Analysis* 34(1), 75-92.

622 Yin J., Ye M., Yin Z. and Xu S. (2015). A review of advances in urban flood risk analysis over
623 China. *Stochastic Environmental Research and Risk Assessment* 29(3), 1063-70.

624 Zaboronski P. C. O. and Zhang K. (2008). *Pricing Options Using Trinomial Trees*, University of
625 Warwick.

626 Zhang C., Wang Y., Li Y. and Ding W. (2017). Vulnerability Analysis of Urban Drainage Systems:
627 Tree vs. Loop Networks. *Sustainability* 9(3), 397.

628 Zhao T., Sundararajan S. K. and Tseng C.-L. (2004). Highway development decision-making
629 under uncertainty: A real options approach. *Journal of Infrastructure Systems* 10(1), 23-32.

630 Zhou Q., Mikkelsen P. S., Halsnæs K. and Arnbjerg-Nielsen K. (2012). Framework for economic
631 pluvial flood risk assessment considering climate change effects and adaptation benefits. *Journal of*
632 *Hydrology* 414(2012), 539-49.

633